horticulturae

MDPI

Article

Genome-Wide Identification of Fatty Acyl-CoA Reductase (FAR) Genes in *Dendrobium catenatum* and Their Response to Drought Stress

Yutong Ren [1,†], Peng Wang [1,2,†], Tingting Zhang [3,†], Wen Liu [1], Yujuan Wang [2], Jun Dai [2,4,*] and Yang Zhou [1,*]

[1] Key Laboratory for Quality Regulation of Tropical Horticultural Crops of Hainan Province, School of Tropical Agriculture and Forestry (School of Agricultural and Rural Affairs, School of Rural Revitalization), Hainan University, Haikou 570228, China; 15135832380@163.com (Y.R.); wangpeng20211@163.com (P.W.); liuwen@hainanu.edu.cn (W.L.)

[2] Anhui Engineering Laboratory for Conservation and Sustainable Utilization of Traditional Chinese Medicine Resources, West Anhui University, Lu'an 237012, China; wangyujuanwyj@126.com

[3] Xiangyang Academy of Agricultural Sciences, Xiangyang 441057, China; 18327852733@163.com

[4] Hainan Sheng Rong Biotechnology Co., Ltd., Haikou 571157, China

* Correspondence: wxxydaijun@163.com (J.D.); zhouyang@hainanu.edu.cn (Y.Z.)

† These authors contributed equally to this work.

Abstract: *Dendrobium catenatum* is a high-value medicinal plant that is predominantly found in high mountain areas, thriving amidst cliffs and rock crevices. However, its wild resources face constant threats from adverse environmental conditions, especially drought stress. Fatty acyl-CoA reductase (FAR) is crucial in plant drought resistance, but there is a lack of research on *FAR* genes in *D. catenatum*. In this study, the FAR family genes were identified from the *D. catenatum* genome. Their genomic characteristics were investigated using bioinformatics techniques, and their expression patterns in different tissues and under 20% PEG8000 conditions mimicking drought stress were analyzed using quantitative real-time RT-PCR (RT-qPCR). Seven *DcFAR* genes were identified from the *D. catenatum* genome. The encoded amino acids range between 377 and 587 aa, with molecular weights between 43.41 and 66.15 kD and isoelectric points between 5.55 and 9.02. Based on the phylogenetic relationships, the FAR family genes were categorized into three subgroups, each with similar conserved sequences and gene structures. The *cis*-acting elements of the promoter regions were assessed, and the results reveal that the *DcFAR* upstream promoter region contains multiple stress-related elements, suggesting its potential involvement in abiotic stress responses. The RT-qPCR results show distinct expression patterns of *DcFAR* genes in various plant tissues. It was observed that the expression of most *DcFAR* genes was upregulated under drought stress. Among them, the expression levels of *DcFAR2*, *DcFAR3*, *DcFAR5*, and *DcFAR7* genes under drought stress were 544-, 193-, 183-, and 214-fold higher compared to the control, respectively. These results indicate that DcFAR2/3/5/7 might play significant roles in *D. catenatum* drought tolerance. This research offers insight into the function of DcFAR genes and provides theoretical support for breeding drought-resistant *D. catenatum* varieties.

Keywords: *Dendrobium catenatum*; FAR gene family; expression patterns; drought stress

check for updates

Citation: Ren, Y.; Wang, P.; Zhang, T.; Liu, W.; Wang, Y.; Dai, J.; Zhou, Y. Genome-Wide Identification of Fatty Acyl-CoA Reductase (FAR) Genes in *Dendrobium catenatum* and Their Response to Drought Stress. *Horticulturae* **2023**, *9*, 982. https://doi.org/10.3390/horticulturae9090982

Academic Editor: Dimitrios Fanourakis

Received: 6 August 2023
Revised: 23 August 2023
Accepted: 29 August 2023
Published: 31 August 2023

1. Introduction

Plant cuticular wax, a fundamental component of the plant epidermis, can prevent water evaporation from the epidermis and acts as the first barrier against both biotic (e.g., pathogenic microbes and pests) and abiotic stresses (e.g., high temperature and drought) [1,2]. A recent research study found that leaf wax could protect rapeseed from infecting *Sclerotinia* [3]. A multitude of studies have reported a significant relationship between cuticle wax content and non-stomatal water loss. Higher wax content can effectively

inhibit plant non-stomatal transpiration, thereby improving plant drought resistance [4]. Muller et al. [5] found that intracuticular waxes, but not epicuticular waxes, play a role in regulating cuticular transpiration. In addition, wax can protect plants from UV radiation to some extent [6,7] and prevent fusion between different plant organs [8], along with inhibiting insect adhesion [9,10].

Plant wax comprises very-long-chain fatty acids (VLCFAs) and their derivatives, including aldehydes, alkanes, ketones, alcohols, and esters. The synthesis pathway of cuticular wax in the epidermis primarily involves three stages: firstly, in plant epidermal mitochondria, acetyl-CoA is extended to form C16 or C18 acyl-acyl carrier protein (acyl-ACP) through the catalytic action of the fatty acid synthase complex (FAS). The resultant acyl-ACP is then hydrolyzed by acyl-ACP thioesterase to form free C16 or C18 fatty acids. Subsequently, in the endoplasmic reticulum, it continues to extend to form VLCFAs with a sufficient carbon chain length (20~34) [11]. Thereafter, aliphatic wax components are synthesized via the alcohol formation (acetyl reduction) pathway and the alkane formation pathway, generating primary alcohols and wax esters via the first pathway, and aldehydes, alkanes, secondary alcohols, and ketones via the second pathway [12,13]. Fatty acyl-CoA reductase (FAR) catalyzes the reduction of fatty acyl-CoA or fatty acyl carrier protein substrates, leading to the formation of primary alcohols [14,15]. In addition, FAR can reduce VLCFA-CoA to aldehydes [16], thus participating in wax synthesis.

FAR exists in both animals and plants, with two conserved domains: the N-terminal NAD(P)(+) binding domain and the C-terminal sterile protein domain [15,17,18]. The N-terminal NAD(P)H domain contains two conserved sequences: the GXXGXX(G/A) sequence and the YXXXK sequence [19–21]. Existing studies have revealed that FAR participates in plant responses to environmental stresses. For instance, under water-deficient conditions, plants may increase wax synthesis by upregulating the expression of key genes for cuticular wax biosynthesis [22]. Wang et al. [23] measured the expression of *TaFAR5* by exposing wheat to drought conditions, finding that drought stress could induce *TaFAR5* expression, thus suggesting its predominant role in plant responses to drought. Moreover, TaFAR1 participates in primary alcohol synthesis, but if overexpressed, it causes an increase in the wax content of wheat leaves, indicating the importance of this gene for researching and breeding drought-resistant wheat [24]. TaFAR2, TaFAR3, and TaFAR4 participate in the synthesis of primary alcohols (C18:0, C28:0, and C24:0, respectively) in wheat leaves. They can respond to low temperatures, drought, and other stresses [24]. In *Brachypodium distachyon*, the BdFAR transcription level increases under drought conditions, suggesting the positive regulation of its transcription in response to drought stress. Nevertheless, observation of the dynamic changes in cuticle wax coverage revealed the role of BdFAR1, BdFAR2, and BdFAR3 in drought-induced cuticle wax accumulation [25]. Similarly, in *Arabidopsis*, drought can stimulate the expression of three wax-biosynthesis-related genes, *FAR4*, *KCS6* (ketoacyl-CoA synthase), and *CER1* (ECERIFERUM1), thereby affecting epidermal wax accumulation and causing changes in wax components [26–28].

Dendrobium catenatum Lindl., a member of the Orchidaceae family, is a valuable medicinal plant with various health benefits, such as heat clearing, detoxification, immune regulation, and anti-tumor properties [29]. *D. catenatum* prefers damp and cool environments and often attaches itself to semi-shaded rocks, tree trunks, or cliffs in the wild. During growth, wild *D. catenatum* is affected by abiotic stress, especially drought stress [30,31], leading to it approaching endangerment [32]. Therefore, identifying drought-resistant genes from *D. catenatum* is crucial for improving drought resistance through molecular breeding techniques. Our research group has previously discovered several drought-related transcription factors in *D. catenatum* [33–37], which serve as candidate genes for studying drought resistance in *D. catenatum*. Within plants, the CBL-CIPK signaling pathway has a significant role in responding to abiotic stress. Zhang et al. [38] identified the abiotic-stress-related CBL-CIPK signaling pathway in *D. catenatum* and found that DcCIPK24 could enhance resistance to drought in transgenic *Arabidopsis* [39]. RNA-seq analysis on transgenic *Arabidopsis* suggested an enrichment of differential genes in the wax biosynthesis pathway

under drought stress as well as prominent upregulation of fatty acyl-CoA reductase 3 (*FAR3*) gene expression in transgenic *Arabidopsis*. Therefore, FAR protein is speculated to be critical in responding to drought stress. However, there is a dearth of research on *FAR* genes in *D. catenatum*. The role of DcFAR protein under drought stress is also unknown. This study aims to perform an identification analysis of *FAR* genes in *D. catenatum* and study their characteristic structures and drought-stress response expression patterns. The aim of this research is to screen drought-stress-associated *DcFAR* genes, guide the study of the regulation of DcCIPK24 drought-resistance functions by FAR protein in *D. catenatum*, and identify candidate genes using molecular biology techniques to improve the resistance of *D. catenatum* to drought in the future.

2. Materials and Methods

2.1. Identification and Physicochemical Properties of FAR Genes in D. catenatum

FAR protein sequences were acquired from the *Arabidopsis* genome website (https://www.arabidopsis.org/, assessed on 26 May 2023), followed by a Blastp analysis using AtFAR protein sequences in the *D. catenatum* genome (PRJNA262478) [40]. An E value of e-10 was screened out, and the obtained protein sequences were identified using the protein family (Pfam) database (http://pfam.xfam.org/, assessed on 26 May 2023), retaining sequences that contained the 'FAR_C' domain (PF07993). These were then verified using the Simple Modular Architecture Research Tool (SMART, http://smart.embl.de/smart/batch.pl, assessed on 26 May 2023) and Conserved Domain Database (CDD, https://www.ncbi.nlm.nih.gov/cdd/, assessed on 26 May 2023) databases. Following the elimination of duplicate and incomplete sequences, the DcFAR sequences were obtained. Using TBtools (v1.120) [41] with gene IDs, the coding sequences (CDSs) and protein sequences of FAR were extracted. The amino acid count, isoelectric point, and molecular weight data for DcFAR proteins were analyzed using the online tool Expert Protein Analysis System (ExPASy, https://web.expasy.org/protparam/, assessed on 26 May 2023). Subcellular localization analysis was conducted using Plant-mPLoc online software (Version 2.0, http://www.csbio.sjtu.edu.cn/cgi-bin/PlantmPLoc.cgi, assessed on 20 August 2023).

2.2. Phylogenetic Analyses of FAR Family Members

FAR protein sequences were retrieved from the *Arabidopsis* genome website (https://www.arabidopsis.org/, assessed on 26 May 2023), and FAR protein sequences from rice and two FAR protein sequences from sorghum were acquired from the NCBI database [23]. These were compared to DcFAR proteins using the MEGA-X software, and a phylogenetic tree was constructed using the Neighbor-Joining (NJ) method, setting the bootstrap value at 1000. Sequence alignment between DcFAR and AtFAR proteins was conducted using DNAMAN software (version 6).

2.3. Conserved Motif and Gene Structure Analyses of DcFARs

Evolutionary analysis was performed on the DcFAR protein sequences using MEGA X software, and an nwk file was exported. The MEME online tool (http://meme-suite.org/, assessed on 7 June 2023) was utilized to assess the conserved motifs of DcFAR proteins, setting the output value at 10, and an XML file was downloaded. TBtools was utilized to retrieve the gene structure data of *FAR* genes from the gff annotation document of the *D. catenatum* genome. Subsequently, visualization analyses of DcFAR protein conserved motifs and gene structures were performed using TBtools.

2.4. Prediction of Cis-Regulatory Elements (CREs) for D. catenatum FAR Gene Promoters

The 2000 bp sequence upstream of the *DcFAR* gene start codon was extracted using TBtools, which served as the gene promoter sequence. The *cis*-acting elements were assessed utilizing the PlantCARE tool (http://bioinformatics.psb.ugent.be/webtools/plantcare/html/, assessed on 4 June 2023), and the outcomes were visualized and quantified for various acting elements by means of TBtools.

2.5. Expression Analysis of DcFAR Genes under Drought Stress

D. catenatum 'Guangnan' was utilized in this research to test the changes in gene expression levels under drought stress. The tissue culture seedlings were cultivated on 1/2 MS medium and maintained under controlled conditions with a cycle of 12 h during the day at 25 °C and 12 h during the night at 22 °C, along with a relative humidity of 70%, within a growth chamber. After three months of growth, uniform and robust plantlets were selected and exposed to drought stress by treating them with 20% PEG8000 to mimic drought stress [33]. The roots, stems, and leaves were collected at various time points (0, 3, 6, 9, 12, 24, and 48 h) after the initiation of the drought treatment [34]. Three biological replicates were used in the assessment. Total RNA extraction and cDNA synthesis followed the methods outlined in a previous study [33]. Quantitative real-time RT-PCR (RT-qPCR) was employed to analyze the expression patterns of *DcFAR* genes, with *DcActin* serving as the internal control. The relative expression levels of *DcFAR* genes were determined using the $2^{-\Delta\Delta CT}$ method [33]. For data presentation, the expression levels under drought stress were divided by those under normal conditions at corresponding time points. The data were analyzed using Excel 2023. The results were expressed as the mean ± standard error (SE) of three replicates, and statistical differences were assessed using Student's *T*-test. Asterisks (* or **) denote significant differences at $p < 0.05$ or 0.01, respectively. The primers utilized in this research are listed in Supplementary Table S1.

2.6. Expression Analysis of DcFAR Genes in Different Tissues

Samples of roots, stems, leaves, capsules, sepals, petals, gynostemia, flower stalks, and lips were collected from two-year-old 'Guangnan' *D. catenatum* plants. The samples were quickly frozen in liquid nitrogen, followed by RNA extraction and synthesis of the first strand of cDNA [33]. The obtained cDNA was used to analyze the expression patterns of *DcFAR* genes in different tissues. The $2^{-\Delta\Delta CT}$ method was employed to calculate changes in the *DcFAR* gene expression levels, and relative expression was calculated by dividing the gene expression levels in various organs by the level in roots. Three independent biological replicates were performed, and the mean expression levels were visualized using TBtools.

3. Results

3.1. Identification and Physicochemical Properties of FAR Genes in D. catenatum

After the identification of the FAR conserved structural domain and confirmation using SMART, Pfam, and CDD databases, seven members of the FAR family were obtained from the *D. catenatum* genome and named *DcFAR1~DcFAR7* according to their gene IDs (Table 1). The amino acid count encoded by these *DcFAR* genes ranges from 377 to 587, with molecular weights ranging between 43.41 and 66.15 kD. Among the *DcFAR* genes, DcFAR6 has the lowest number of encoded amino acids and the smallest molecular weight, while DcFAR2 has the highest number of encoded amino acids and the largest molecular weight. The theoretical isoelectric point of the DcFAR proteins ranges from 5.55 to 9.02. Subcellular localization predictions indicate that these proteins are located in different parts of plant cells. DcFAR1 is located in the Golgi apparatus, while DcFAR2 and DcFAR6 are located in chloroplast, thus belonging to plastid-localized proteins. DcFAR3 localizes in the cytoplasm, DcFAR5 localizes in both chloroplast and the Golgi apparatus, and the DcFAR7 protein localizes in mitochondrion.

Table 1. Physicochemical properties of FAR gene family in *D. catenatum*.

Gene Name	Gene ID	Number of AA	Molecular Weight (kDa)	Isoelectric Point	Subcellular Localization
DcFAR1	LOC110092925	489	56.05	9.02	Golgi apparatus
DcFAR2	LOC110103179	587	66.15	9.02	Chloroplast
DcFAR3	LOC110112054	490	56.44	8.83	Cytoplasm
DcFAR4	LOC110114508	489	56.62	6.96	Unidentified
DcFAR5	LOC110114509	407	46.43	5.81	Chloroplast, Golgi apparatus
DcFAR6	LOC110114627	377	43.41	5.55	Chloroplast
DcFAR7	LOC110114642	443	51.14	8.49	Mitochondrion

3.2. Phylogenetic Analyses of FAR Family Members of D. catenatum and Other Plant Species

Using MEGA-X, a phylogenetic tree was constructed using the NJ method for FAR proteins from *D. catenatum*, *Arabidopsis*, rice, and sorghum (Figure 1A, Supplementary Table S2). The results suggest that FARs can be categorized into three groups: groups A, B, and C. DcFARs only exist in groups A and C. In group A, DcFAR2 clusters on the same evolutionary branch with AtFAR2 and AtFAR6 from *Arabidopsis*. Group B only contains seven *Arabidopsis* FAR members. Group C has the largest evolutionary branch, including six DcFARs, seven OsFAR proteins, and two SbFAR proteins. These results indicate that the evolutionary relationship of FAR proteins in different plant species is far, whereas the genetic relationship of FAR proteins in the same plant is close. DcFARs from *D. catenatum* are aligned with three *Arabidopsis* FARs and one rice FAR protein. These results indicate that all FAR proteins have two conserved domains, GXXGXX(G/A) and YXXXK, where DcFAR2, DcFAR6, and DcFAR7 contain one YXXXK conserved domain, while the remaining proteins all contain two YXXXK conserved domains (Figure 1B).

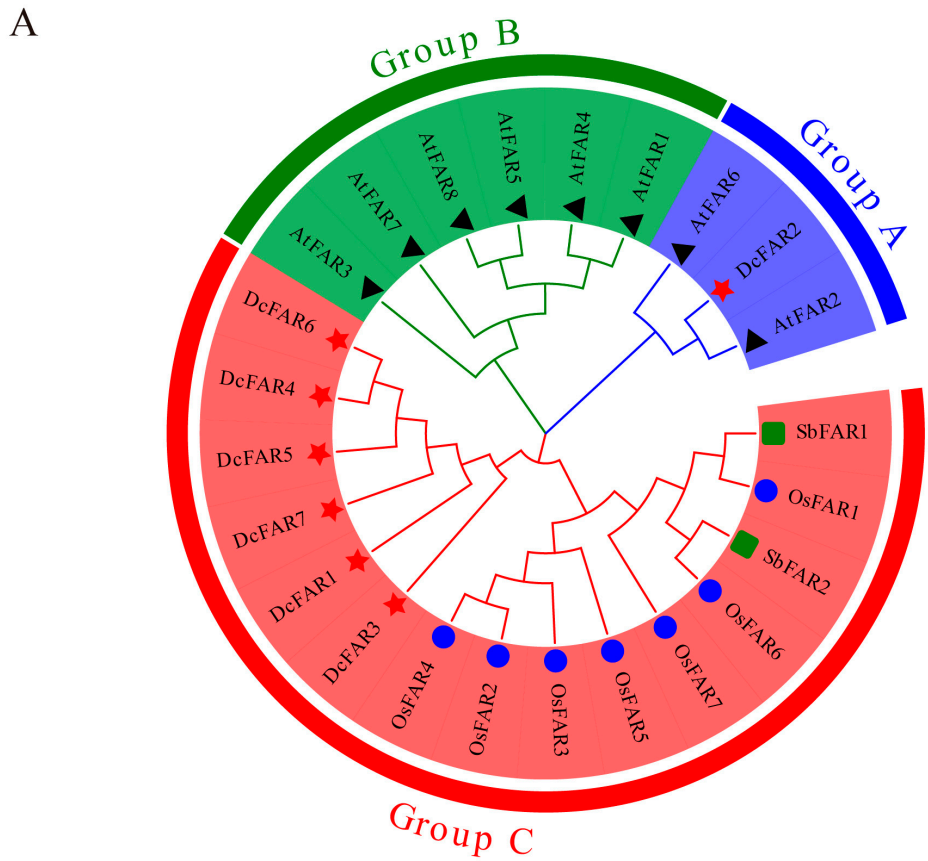

Figure 1. *Cont.*

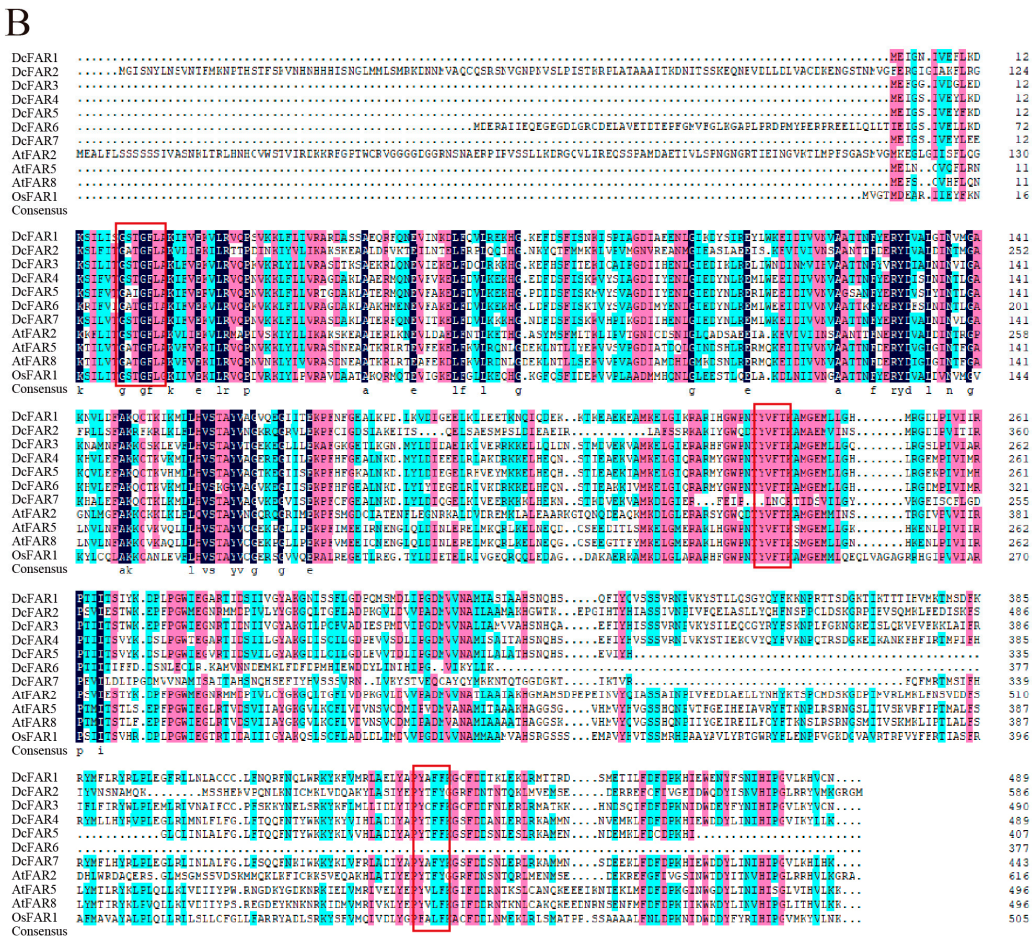

Figure 1. Phylogenetic analysis and protein sequence comparison of FAR proteins. (**A**) Phylogenetic analysis of FAR proteins from *D. catenatum*, *Arabidopsis*, rice, and sorghum. The phylogenetic tree was constructed using the Neighbor-Joining (NJ) method in MEGA-X, with default parameters. Red star represents *D. catenatum* FAR (DcFAR); black triangle represents *Arabidopsis* FAR (AtFAR); green square represents sorghum FAR; and blue circle represents rice FAR (OsFAR). (**B**) Protein sequence comparison of FAR proteins using DNAMAN. The three red boxes represent the GXXGXX(G/A) and YXXXK conserved domains.

3.3. Conserved Motif and Gene Structure Analyses of FAR Family Members

Among the predicted ten conserved motifs (Supplementary Figure S1), except for DcFAR2 and DcFAR7, all other DcFAR proteins contain the motif structure motif3–motif4–motif1–motif7–motif2. DcFAR2 lacks motif7, and DcFAR7 lacks motif2. Motif6 exists in all DcFAR proteins except DcFAR6; motif8 exists in all DcFAR proteins except DcFAR5; motif9 exists in all DcFAR proteins except DcFAR5 and DcFAR6; and motif10 exists in all DcFAR proteins except DcFAR2, DcFAR5, and DcFAR6 (Figure 2A, Supplementary Table S3). Observation of the gene structure revealed that the intron count in *DcFAR* genes is eight or nine. Among them, *DcFAR2* and *DcFAR7* have eight introns, while the other genes contain nine introns (Figure 2B, Supplementary Table S3).

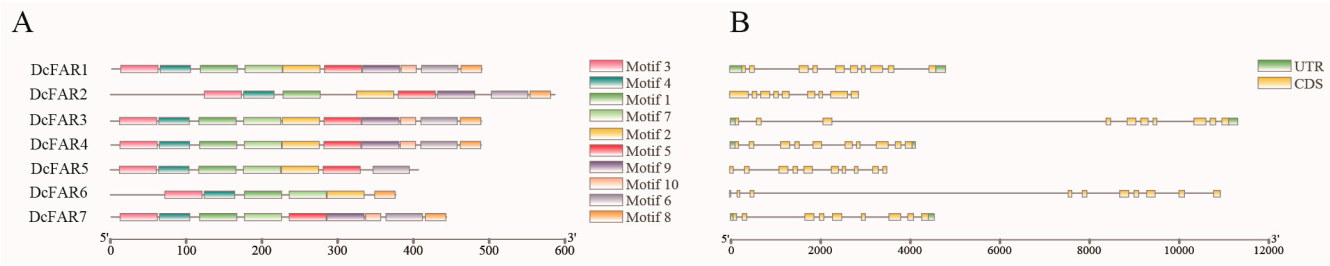

Figure 2. Conserved motif and gene structure analyses of DcFAR family members. (**A**) Conserved motifs of DcFAR proteins. Rectangular boxes of different colors represent different conserved motifs. (**B**) Exon/intron structure of *DcFAR*. UTR(s), exon(s), and intron(s) are represented by green boxes, yellow boxes, and black lines, respectively.

3.4. Prediction of Cis-Regulatory Elements (CREs) for D. catenatum FAR Gene Promoters

The promoter sequences of the *DcFAR* genes in *D. catenatum* were analyzed using the PlantCARE online website, considering the 2000 bp sequence upstream of the gene start codon. This analysis revealed the presence of 24 *cis*-acting elements in the promoter region (Figure 3A). The identified *cis*-acting elements in the promoter region are sorted into four distinct groups: hormone response elements, stress related elements, plant-growth-and-development-related elements, and light response elements. Among these, hormone response elements include abscisic acid (ABA) response element (ABRE), auxin (IAA) response element (TGA-element), salicylic acid (SA) response element (TCA-element), gibberellin (GA) response element (P-box), and methyl jasmonate (MeJA) response element (CGTCA-motif/TGACG-motif). The plant-growth-and-development-related elements found in the *DcFAR* gene promoter of *D. catenatum* mainly consist of meristem-expression-related elements (CAT-box) and zein metabolism regulatory elements (O2-site). The light response elements include AE-box, TCT-motif, Box 4, and GATA-motif. Additionally, the stress related elements encompass wound response (WUN-motif), low temperature response (LTR), drought induction (MBS), and stress and defense response elements (TC-rich repeats). In the analysis, LTR was detected in four *DcFAR* gene promoters, MBS was found in three *DcFAR* gene promoters, TC-rich repeat elements were present in two *DcFAR* gene promoters, and WUN-motif was identified in one *DcFAR* gene promoter (Figure 3B). These findings indicate that *DcFAR* is widely involved in response to various abiotic stresses.

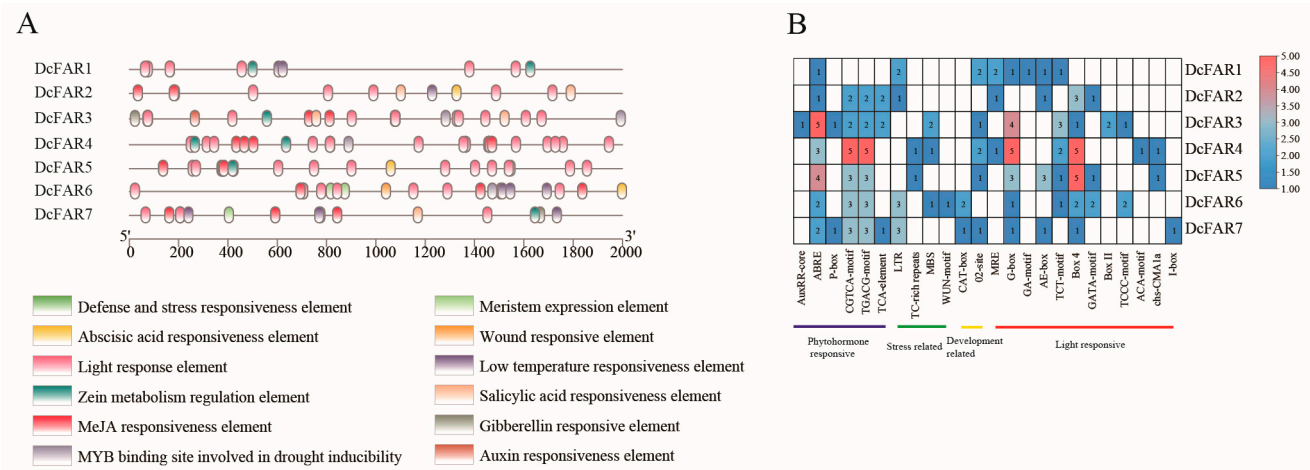

Figure 3. *Cis*-acting element analysis in the promoter of *DcFAR* genes. (**A**) Locations of *cis*-acting elements in the promoter of *DcFAR*. Ellipses of different colors represent different types of *cis*-acting elements and their positions in each *DcFAR* gene promoter. (**B**) Statistics of the number of *cis*-acting elements in *DcFAR* promoters. Different colors and numbers represent the number of different *cis*-acting elements in each *DcFAR* promoter.

3.5. Expression Analysis of DcFAR Genes under Drought Stress

The levels of *DcFAR* gene expression under drought stress conditions were assessed utilizing the RT-qPCR method. As illustrated in Figure 4, most *DcFAR* genes showed varying levels of upregulation under drought conditions. *DcFAR2*, *DcFAR3*, and *DcFAR6* were considerably upregulated in the roots after the drought-stress treatment. After 12 h of drought treatment, the highest *DcFAR2* expression level was observed in roots, which was 544 times higher than the level observed in the control group. The relative expression levels of *DcFAR3* and *DcFAR6* after 6 h of stress treatment were 193 and 40 times the initial expression levels, respectively. In leaves, *DcFAR1*, *DcFAR4*, and *DcFAR7* were markedly upregulated after the drought-stress treatment. The relative expression levels of *DcFAR1* and *DcFAR4* after 9 h of stress treatment were 34 and 43 times the initial levels, respectively. After 24 h of drought-stress treatment, the relative expression level of *DcFAR7* reached 214 times its initial expression. In stems, the relative expression levels of *DcFAR4* and *DcFAR5* after 48 h of stress treatment were 59 and 183 times their initial expression levels, respectively, while the expression of other genes remained relatively unchanged.

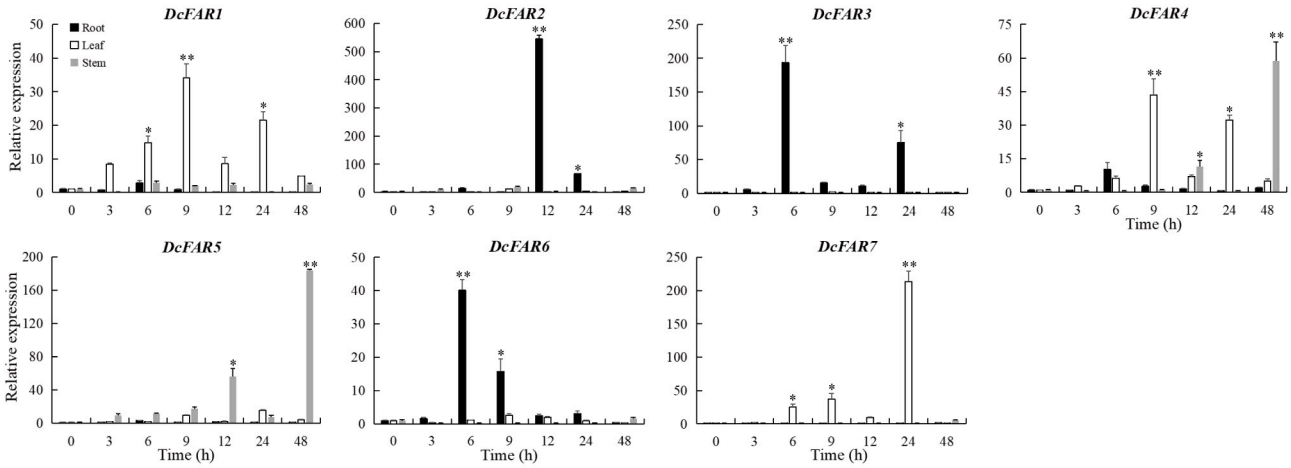

Figure 4. Expression analysis of *DcFAR* genes under drought stress using RT-qPCR. The data are expressed as mean ± standard deviation (n = 3). Vertical bars represent the means of fold change in expression and standard deviations calculated from the replicates. Values of 0, 3, 6, 9, 12, 24, and 48 indicate hours after treatment. Asterisks (* or **) indicate a significant difference at $p < 0.05$ or 0.01, respectively.

3.6. Expression Analysis of FAR Genes in Different Tissues

Samples were collected from nine tissues of *D. catenatum*, including roots, stems, leaves, capsules, sepals, petals, gynostemia, flower stalks, and lips, and the degree of *DcFAR* expression in these organs was measured. As demonstrated in Figure 5 and Supplementary Table S4, the seven *DcFAR* genes showed differences in their expression levels among different tissues. *DcFAR* genes were primarily expressed in reproductive organs. *DcFAR3* was highly expressed in most organs. *DcFAR1*, *DcFAR4*, and *DcFAR6* were mainly expressed in capsules, with *DcFAR1* having the highest expression level, which was 168 times higher than that in roots. The highest expression level of *DcFAR2* was in flower stalks. The expression levels of *DcFAR3* and *DcFAR5* in petals were 740 and 70 times higher than those in roots, respectively. However, *DcFAR7* exhibited relatively low expression in all organs.

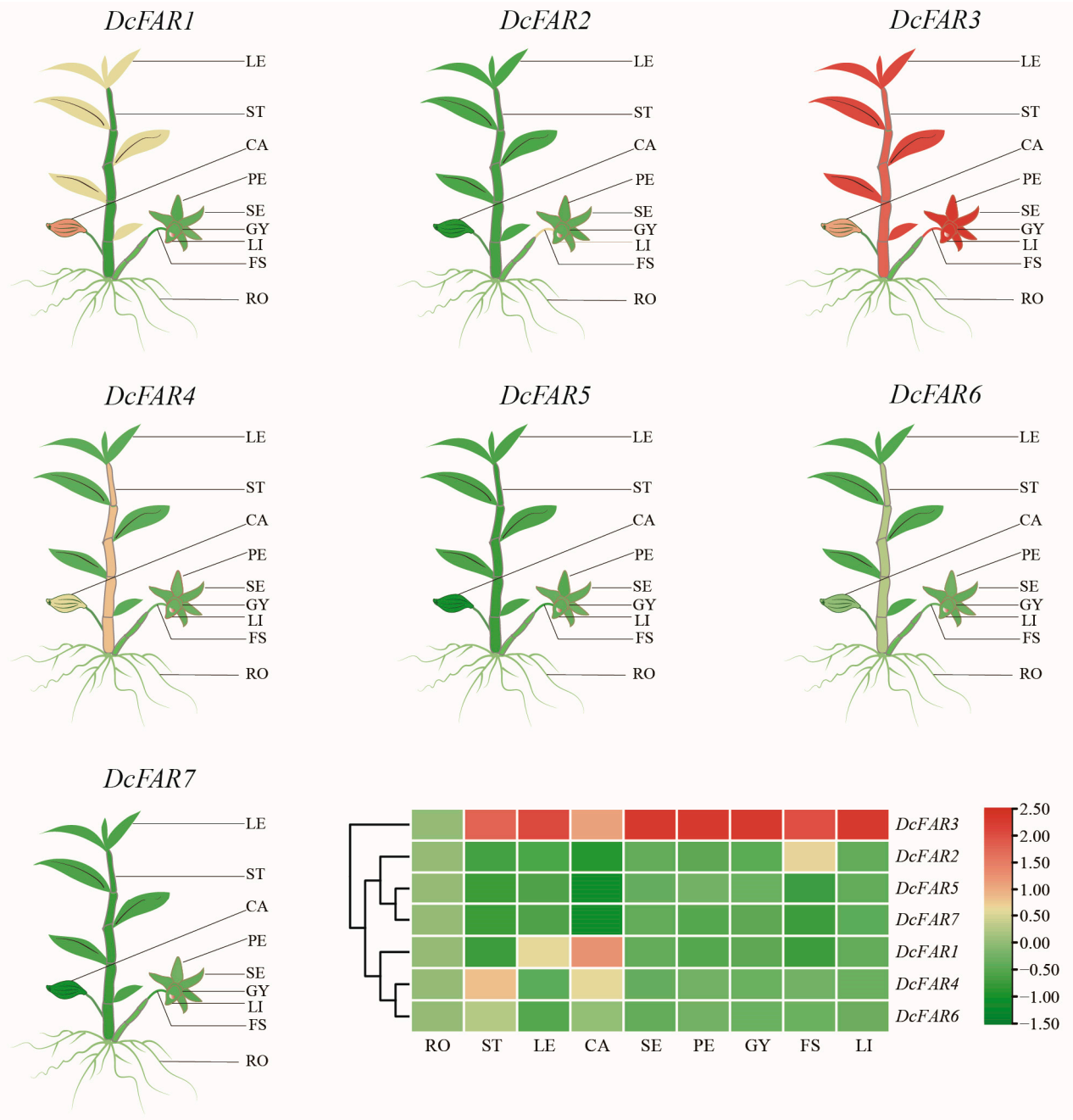

Figure 5. Expression analysis of *DcFAR* genes in different tissues using RT-qPCR. Mean expression values were calculated from three independent biological replicates relative to the value in roots and visualized using TBtools. Green and red indicate low and high levels of expression, respectively. RO: root; ST: stem; LE: leaf; CA: capsule; E: petal; SE: sepal; FS: flower stalk; GY: gynostemia; LI: lip.

4. Discussion

FAR proteins play a significant role in protection against UV radiation and resistance to biotic and abiotic stresses [1,2,6–8]. *FAR* genes have been identified in *Arabidopsis* [42], wheat [23,24,43,44], ryegrass [25], corn [45], cotton [46], and rice [47]. The results of these studies suggest that FAR mediates the response to drought stress in plants. However, previous studies failed to comprehensively assess the gene characteristics of the FAR family in *D. catenatum* and their role in drought response. In this study, bioinformatics technology was used to identify seven *DcFAR* genes from the genome of *D. catenatum*. Additionally, this research assessed the physicochemical properties, phylogenetic relationships, conserved

motifs, *cis*-acting elements in promoter regions, gene structures, and expression patterns of the identified *DcFAR* genes under drought stress conditions and in different tissue parts.

The average molecular weight of these DcFAR proteins is approximately 54 kD, which is close to the reported molecular weights of FAR proteins in jojoba [16] and pea [48]. According to phylogenetic analysis, the FAR gene family can be sorted into three subgroups: groups A, B, and C (Figure 1), which is in accordance with the findings of Schwacke et al. [49]. Among them, group A has the fewest members, while group C has the most members. Apart from DcFAR2, all other proteins are clustered in group C. Similarly, ten GhFARs of cotton mostly cluster in the same subgroup [46]. FAR proteins have distinct substrate specificities, which are directly connected to their diversity in subcellular localizations [50]. Previous studies have revealed that AtFAR2/MS2 is located in plastids [51]. Its specifically recognized substrate is C16:0-ACP, and the final catalytic product is C16:0 primary alcohol, which is mainly involved in the synthesis of the tapetum of pollen wall in *Arabidopsis* [21,52]. AtFAR1, AtFAR4, and AtFAR5 proteins are primarily responsible for the production of C22:0-, C20:0-, and C18:0-OH, respectively [26]. The phylogenetic relationship analysis showed that DcFAR2 has a high homology with AtFAR2/MS2 (Figure 1A). Thus, DcFAR2 is inferred to have similar functions. Subcellular localization prediction showed that DcFAR2 is mainly located in chloroplast, similar to AtFAR2 [51], showing that both are plastid-localized proteins. Plant FARs often divide into microsomal-localized and plastid-localized proteins [50]. Unlike microsomal–localized FARs, plastid-localized FARs not only contain GXXGXX(G/A) and YXXXK conserved domains but also an N-terminal extension (plastid transit peptide) [45,51,53,54]. The protein sequence alignment suggests that all DcFAR proteins contain two conserved domains, GXXGXX(G/A) and YXXXK, which are shared by FARs [19–21], indicating DcFARs' relative conservation during evolution. Among them, DcFAR2 contains only one YXXXK conserved domain, aligning with the observations obtained from the phylogenetic tree analysis. In addition, sequence alignments showed that both DcFAR2 and AtFAR2 have an extended N-terminus (Figure 1B), which might be a plastid transit peptide [50]. These findings suggest that DcFAR2 has a relatively distant relationship with other DcFARs.

Gene structure is crucial for the study of gene evolutionary relationships [55]. Previous research has demonstrated that the *Arabidopsis CER4/FAR3* gene contains nine introns [56], while the wheat *TaFAR1* gene contains seven introns [43]. This study found that there are eight or nine introns in *DcFAR* genes (Figure 2B), similar to the numbers in *Arabidopsis CER4* and wheat *TaFAR1.* Moreover, the conserved motifs of most FAR proteins exhibit similar patterns, except that DcFAR2 lacks motif7, and DcFAR7 lacks motif2; all other DcFAR proteins contain the conserved motif structure motif3–motif4–motif1–motif7–motif2. Both analyses of conserved motifs and gene structures suggest that *DcFAR* genes are highly conserved during evolution.

The function of a gene is linked with its expression pattern [57]. The expression of *DcFAR* genes shows tissue-specific differences. According to the spatial expression patterns, *DcFAR* genes can be divided into three types (Figure 5): the first type mainly expresses in capsules, including *DcFAR1*, *DcFAR4*, and *DcFAR6*; the second type mainly expresses in petals and flower stalks, including *DcFAR2*, *DcFAR3*, and *DcFAR5*; and the third type mainly expresses in roots, including *DcFAR7*. *Arabidopsis FAR2/MS2* primarily expresses in flowers, participating in the biosynthesis of sporopollenin [21,52], whereas *DcFAR2* also significantly expresses in flowers. The phylogenetic analysis showed that both AtFAR2 and DcFAR2 belong to group A, suggesting their similar functions. Compared to other *DcFAR* genes, *DcFAR3* expresses at a high level in all tissues, indicating its significant regulatory effect on various organs of *D. catenatum*. A relatively low expression of *DcFAR7* in all tissues of *D. catenatum* is worth noting. Its low expression levels in the tested tissues might be affected by the combination/kind of *cis*-acting elements in the promoter region (Figure 3B).

D. catenatum often grows on cliffs and rock crevices. All through its life, it often faces threats from harsh environmental conditions, especially drought stress. FAR is the key enzyme for the synthesis of plant waxes and is closely linked with plant resistance to biotic

and abiotic stresses [1,2]. This study used the RT-qPCR technique to study the expression patterns of seven *DcFAR* genes during drought conditions. The results revealed a significant upregulation of *DcFAR2* and *DcFAR3* in roots, *DcFAR5* in stems, and *DcFAR7* in leaves under drought stress (Figure 4). Previous research revealed that *cis*-acting elements in the promoter region can bind with target genes, leading to the induction of their expression under abiotic stress [58,59]. In the analysis of *cis*-acting elements in the promoter region, the drought-induced element MBS was detected in the *DcFAR3* gene promoter, indicating its ability to induce *DcFAR3* expression under drought stress. Furthermore, jasmonic acid (JA) and salicylic acid (SA) are crucial signaling molecules in plants [60,61] and can activate the expression of stress-resistance genes in plants. Most *DcFAR* genes contain methyl jasmonate (MeJA) response elements and salicylic acid (SA) response elements, implying the possible involvement of these genes in SA and JA-mediated signal transduction pathways [62,63]. However, their functions must be assessed with additional research.

5. Conclusions

In the current research, seven *DcFAR* genes from *D. catenatum* were identified, and their genomic features were investigated. RT-qPCR analysis revealed tissue-specific expression patterns of *DcFAR*s. An analysis study of the expression patterns of *DcFAR* genes during drought conditions found that most *DcFAR* genes are induced by drought stress, among which *DcFAR2*, *DcFAR3*, *DcFAR5*, and *DcFAR7* are most significantly upregulated in roots, stems, and leaves, respectively. Further studies are needed to study their functions and regulation of drought tolerance. These results provide insights into the molecular breeding of drought-resistant *D. catenatum*.

Supplementary Materials: The following supporting information can be downloaded at: https://www.mdpi.com/article/10.3390/horticulturae9090982/s1, Figure S1: Sequence of each motif; Table S1: Primers used in this study; Table S2: The gene ID of FARs in *D. catenatum*, *A. thaliana*, *O. sativa*, and *S. bicolor*; Table S3: Motifs and the number of introns of each *DcFAR* gene; Table S4: Expression data of *DcFAR* genes in different tissues of *D. catenatum*.

Author Contributions: Conceptualization, J.D. and Y.Z.; formal analysis, Y.R., P.W., T.Z., W.L., Y.W. and Y.Z.; funding acquisition, J.D. and Y.Z.; investigation, Y.R., P.W., T.Z., W.L., Y.W. and Y.Z.; methodology, Y.R. and T.Z; supervision, Y.Z; writing—original draft preparation, Y.R. and Y.Z.; writing—review and editing, J.D. and Y.Z. All authors have read and agreed to the published version of the manuscript.

Funding: This research was funded by the Hainan Province Science and Technology Special Fund (ZDYF2023SHFZ122), the Haikou Science and Technology Planning Project (2022-008, 2022-011), the Hainan Provincial Natural Science Foundation of China (319MS009), the Education Department of Hainan Province (Hnky2021-19), the Horizontal Project of Hainan University (HD-KYH-2023093), and the Key Project of Scientific Research in Higher Education of Anhui Province (2022AH051677).

Data Availability Statement: Not applicable.

Acknowledgments: We thank the reviewers and editors for helpful comments on earlier drafts of the manuscript.

Conflicts of Interest: The authors declare no conflict of interest.

References

1. Lewandowska, M.; Keyl, A.; Feussner, I. Wax biosynthesis in response to danger: Its regulation upon abiotic and biotic stress. *New Phytol.* **2020**, *227*, 698–713. [CrossRef] [PubMed]
2. Martin, L.B.; Rose, J.K. There's more than one way to skin a fruit: Formation and functions of fruit cuticles. *J. Exp. Bot.* **2014**, *65*, 4639–4651. [CrossRef] [PubMed]
3. Long, Z.; Tu, M.; Xu, Y.; Pak, H.; Zhu, Y.; Dong, J.; Lu, Y.; Jiang, L. Genome-wide-association study and transcriptome analysis reveal the genetic basis controlling the formation of leaf wax in *Brassica napus*. *J. Exp. Bot.* **2023**, *74*, 2726–2739. [CrossRef]
4. Buschhaus, C.; Jetter, R. Composition and physiological function of the wax layers coating *Arabidopsis* leaves: β-amyrin negatively affects the intracuticular water barrier. *Plant Physiol.* **2012**, *160*, 1120–1129. [CrossRef]

5. Muller, Y.; Patwari, P.; Stocker, T.; Zeisler-Diehl, V.; Steiner, U.; Campoli, C.; Grewe, L.; Kuczkowska, M.; Dierig, M.M.; Jose, S.; et al. Isolation and characterization of the gene *HvFAR1* encoding acyl-CoA reductase from the *cer-za.227* mutant of barley (*Hordeum vulgare*) and analysis of the cuticular barrier functions. *New Phytol.* **2023**, *239*, 1903–1918. [CrossRef] [PubMed]
6. Shepherd, T.; Griffiths, D.W. The effects of stress on plant cuticular waxes. *New Phytol.* **2006**, *171*, 469–499. [CrossRef] [PubMed]
7. Long, L.M.; Patel, H.P.; Cory, W.C.; Stapleton, A.E. The maize epicuticular wax layer provides UV protection. *Funct. Plant Biol.* **2003**, *30*, 75–81. [CrossRef]
8. Sieber, P.; Schorderet, M.; Ryser, U.; Buchala, A.; Kolattukudy, P.; Métraux, J.P.; Nawrath, C. Transgenic Arabidopsis plants expressing a fungal cutinase show alterations in the structure and properties of the cuticle and postgenital organ fusions. *Plant Cell* **2000**, *12*, 721–738. [CrossRef]
9. Gorb, E.V.; Gorb, S.N. Anti-adhesive effects of plant wax coverage on insect attachment. *J. Exp. Bot.* **2017**, *68*, 5323–5337. [CrossRef]
10. Gaume, L.; Perret, P.; Gorb, E.; Gorb, S.; Labat, J.J.; Rowe, N. How do plant waxes cause flies to slide? Experimental tests of wax-based trapping mechanisms in three pitfall carnivorous plants. *Arthropod. Struct. Dev.* **2004**, *33*, 103–111. [CrossRef]
11. Yang, X.P.; Zhao, H.Y.; Kosma, D.K.; Tomasi, P.; Dyer, J.M.; Li, R.; Liu, X.; Wang, Z.; Parsons, E.P.; Jenks, M.A.; et al. The acyl desaturase CER17 is involved in producing wax unsaturated primary alcohols and cutin monomers. *Plant Physiol.* **2017**, *173*, 1109–1124. [CrossRef] [PubMed]
12. Samuels, L.; Kunst, L.; Jetter, R. Sealing plant surfaces: Cuticular wax formation by epidermal cells. *Annu. Rev. Plant Biol.* **2008**, *59*, 683–707. [CrossRef]
13. Kunst, L.; Samuels, L. Plant cuticles shine: Advances in wax biosynthesis and export. *Curr. Opin. Plant. Biol.* **2009**, *12*, 721–727. [CrossRef] [PubMed]
14. Chacón, M.G.; Fournier, A.E.; Tran, F.; Dittrich-Domergue, F.; Pulsifer, I.P.; Domergue, F.; Rowland, O. Identification of amino acids conferring chain length substrate specificities on fatty alcohol-forming reductases FAR5 and FAR8 from *Arabidopsis thaliana*. *J. Biol. Chem.* **2013**, *288*, 30345–30355. [CrossRef] [PubMed]
15. Teerawanichpan, P.; Qiu, X. Fatty acyl-CoA reductase and wax synthase from *Euglena gracilis* in the biosynthesis of medium-chain wax esters. *Lipids* **2010**, *45*, 263–273. [CrossRef]
16. Metz, J.G.; Pollard, M.R.; Anderson, L.; Hayes, T.R.; Lassner, M.W. Purification of a jojoba embryo fatty acyl-coenzyme A reductase and expression of its cDNA in high erucic acid rapeseed. *Plant Physiol.* **2000**, *122*, 635–644. [CrossRef]
17. Doan, T.T.; Carlsson, A.S.; Hamberg, M.; Bülow, L.; Stymne, S.; Olsson, P. Functional expression of five *Arabidopsis* fatty acyl-CoA reductase genes in *Escherichia coli*. *J. Plant Physiol.* **2009**, *166*, 787–796. [CrossRef]
18. Teerawanichpan, P.; Robertson, A.J.; Qiu, X. A fatty acyl-CoA reductase highly expressed in the head of honey bee (*Apis mellifera*) involves biosynthesis of a wide range of aliphatic fatty alcohols. *Insect Biochem. Mol. Biol.* **2010**, *40*, 641–649. [CrossRef]
19. Marchler-Bauer, A.; Lu, S.; Anderson, J.B.; Chitsaz, F.; Derbyshire, M.K.; DeWeese-Scott, C.; Fong, J.H.; Geer, L.Y.; Geer, R.C.; Gonzales, N.R.; et al. CDD: A Conserved Domain Database for the functional annotation of proteins. *Nucleic Acids Res.* **2011**, *39*, 225–229. [CrossRef]
20. Kallberg, Y.; Oppermann, U.; Persson, B. Classification of the short-chain dehydrogenase/reductase superfamily using hidden Markov models. *FEBS J.* **2010**, *277*, 2375–2386. [CrossRef]
21. Aarts, M.G.; Hodge, R.; Kalantidis, K.; Florack, D.; Wilson, Z.A.; Mulligan, B.J.; Stiekema, W.J.; Scott, R.; Pereira, A. The *Arabidopsis* MALE STERILITY 2 protein shares similarity with reductases in elongation/condensation complexes. *Plant J.* **1997**, *12*, 615–623. [CrossRef] [PubMed]
22. Hooker, T.S.; Millar, A.A.; Kunst, L. Significance of the expression of the CER6 condensing enzyme for cuticular wax production in *Arabidopsis*. *Plant Physiol.* **2002**, *129*, 1568–1580. [CrossRef] [PubMed]
23. Wang, Y.; Wang, M.; Sun, Y.; Wang, Y.; Li, T.; Chai, G.; Jiang, W.; Shan, L.; Li, C.; Xiao, E.; et al. FAR5, a fatty acyl-coenzyme A reductase, is involved in primary alcohol biosynthesis of the leaf blade cuticular wax in wheat (*Triticum aestivum* L.). *J. Exp. Bot.* **2015**, *66*, 1165–1178. [CrossRef] [PubMed]
24. Wang, M.; Wang, Y.; Wu, H.; Xu, J.; Li, T.; Hegebarth, D.; Jetter, R.; Chen, L.; Wang, Z. Three *TaFAR* genes function in the biosynthesis of primary alcohols and the response to abiotic stresses in *Triticum aestivum*. *Sci. Rep.* **2016**, *6*, 25008. [CrossRef] [PubMed]
25. Wang, Y.; Sun, Y.; You, Q.; Luo, W.; Wang, C.; Zhao, S.; Chai, G.; Li, T.; Shi, X.; Li, C.; et al. Three fatty acyl-coenzyme A reductases, BdFAR1, BdFAR2 and BdFAR3, are involved in cuticular wax primary alcohol biosynthesis in brachypodium distachyon. *Plant Cell Physiol.* **2018**, *59*, 527–543. [CrossRef] [PubMed]
26. Domergue, F.; Vishwanath, S.J.; Joubès, J.; Ono, J.; Lee, J.A.; Bourdon, M.; Alhattab, R.; Lowe, C.; Pascal, S.; Lessire, R.; et al. Three *Arabidopsis* fatty acyl-coenzyme A reductases, FAR1, FAR4, and FAR5, generate primary fatty alcohols associated with suberin deposition. *Plant Physiol.* **2010**, *153*, 1539–1554. [CrossRef]
27. Denic, V.; Weissman, J.S. A molecular caliper mechanism for determining very long-chain fatty acid length. *Cell* **2007**, *130*, 663–677. [CrossRef]
28. Bernard, A.; Domergue, F.; Pascal, S.; Jetter, R.; Renne, C.; Faure, J.D.; Haslam, R.P.; Napier, J.A.; Lessire, R.; Joubès, J. Reconstitution of plant alkane biosynthesis in yeast demonstrates that *Arabidopsis* ECERIFERUM1 and ECERIFERUM3 are core components of a very-long-chain alkane synthesis complex. *Plant Cell* **2012**, *24*, 3106–3118. [CrossRef]

29. Sun, J.; Guo, Y.; Fu, X.; Wang, Y.; Liu, Y.; Huo, B.; Sheng, J.; Hu, X. Dendrobium candidum inhibits MCF-7 cells proliferation by inducing cell cycle arrest at G2/M phase and regulating key biomarkers. *OncoTargets Ther.* **2015**, *9*, 21–30. [CrossRef]
30. Zotz, G.; Winkler, U. Aerial roots of epiphytic orchids: The velamen radicum and its role in water and nutrient uptake. *Oecologia* **2013**, *171*, 733–741. [CrossRef]
31. Zou, L.H.; Wan, X.; Deng, H.; Zheng, B.Q.; Li, B.J.; Wang, Y. Data descriptor: RNA-seq transcriptomic profiling of crassulacean acid metabolism pathway in *Dendrobium catenatum*. *Sci. Data* **2018**, *5*, 180252. [CrossRef]
32. Ng, T.B.; Liu, J.; Wong, J.H.; Ye, X.; Sze, S.C.W.; Tong, Y.; Zhang, K.Y. Review of research on Dendrobium, a prized folk medicine. *Appl. Microbiol. Biotechnol.* **2012**, *93*, 1795–1803. [CrossRef] [PubMed]
33. Zhang, T.T.; Cui, Z.; Li, Y.; Kang, Y.; Song, X.; Wang, J.; Zhou, Y. Genome-wide identification and expression analysis of MYB transcription factor superfamily in *Dendrobium catenatum*. *Front. Genet.* **2021**, *12*, 714696. [CrossRef]
34. Zhang, T.T.; Xu, Y.; Ding, Y.; Yu, W.; Wang, J.; Lai, H.; Zhou, Y. Identification and expression analysis of WRKY gene family in response to abiotic stress in *Dendrobium catenatum*. *Front. Genet.* **2022**, *13*, 800019. [CrossRef] [PubMed]
35. Li, Y.; Zhang, T.T.; Xing, W.; Wang, J.; Yu, W.; Zhou, Y. Comprehensive genomic characterization of the NAC transcription factors and their response to drought stress in *Dendrobium catenatum*. *Agronomy* **2022**, *12*, 2753. [CrossRef]
36. Wang, P.; Li, Y.X.; Zhang, T.T.; Kang, Y.Q.; Li, W.; Wang, J.; Yu, W.; Zhou, Y. Identification of the bZIP gene family and investigation of their response to drought stress in *Dendrobium catenatum*. *Agronomy* **2023**, *13*, 236. [CrossRef]
37. Yang, T.; Zhang, T.; Li, Y.; Kang, Y.; Wang, P.; Liu, W.; Wang, Y.; Tian, L.; Dai, J.; Zhou, Y. Genome-wide identification and expression analysis of the chalcone synthase (CHS) gene family in *Dendrobium catenatum*. *Agronomy* **2023**, *13*, 1488. [CrossRef]
38. Zhang, T.T.; Li, Y.X.; Wang, P.; Luo, Q.; Fu, S.; Kang, Y.; Zhou, Y. Characterization of *Dendrobium catenatum* CBL-CIPK signaling networks and their response to abiotic stress. *Int. J. Biol. Macromol.* **2023**, *236*, 124010. [CrossRef]
39. Zhang, T.T.; Li, Y.; Kang, Y.; Wang, P.; Li, W.; Yu, W.; Wang, J.; Wang, J.; Song, X.; Jiang, X.Y.; et al. The *Dendrobium catenatum* DcCIPK24 increases drought and salt tolerance of transgenic *Arabidopsis*. *Ind. Crop. Prod.* **2022**, *187*, 115375. [CrossRef]
40. Zhang, G.Q.; Xu, Q.; Bian, C.; Tsai, W.C.; Yeh, C.M.; Liu, K.W.; Yoshida, K.; Zhang, L.S.; Chang, S.B.; Chen, F.; et al. The *Dendrobium catenatum* Lindl. genome sequence provides insights into polysaccharide synthase, floral development and adaptive evolution. *Sci. Rep.* **2016**, *6*, 19029. [CrossRef]
41. Chen, C.; Chen, H.; Zhang, Y.; Thomas, H.R.; Frank, M.H.; He, Y.H.; Xia, R. TBtools: An integrative toolkit developed for interactive analyses of big biological data. *Mol. Plant* **2020**, *13*, 1194–1202. [CrossRef] [PubMed]
42. Gupta, N.C.; Jain, P.K.; Bhat, S.R.; Srinivasan, R. Upstream sequence of fatty acyl-CoA reductase (FAR6) of *Arabidopsis thaliana* drives wound-inducible and stem-specific expression. *Plant Cell Rep.* **2012**, *31*, 839–850. [CrossRef] [PubMed]
43. Wang, Y.; Wang, M.; Sun, Y.; Hegebarth, D.; Li, T.; Jetter, R.; Wang, Z. Molecular Characterization of TaFAR1 involved in primary alcohol biosynthesis of cuticular wax in hexaploid wheat. *Plant Cell Physiol.* **2015**, *56*, 1944–1961. [CrossRef]
44. Chai, G.; Li, C.; Xu, F.; Li, Y.; Shi, X.; Wang, Y.; Wang, Z. Three endoplasmic reticulum-associated fatty acyl-coenzyme a reductases were involved in the production of primary alcohols in hexaploid wheat (*Triticum aestivum* L.). *BMC Plant Biol.* **2018**, *18*, 41. [CrossRef]
45. Zhang, S.; Wu, S.; Niu, C.; Liu, D.; Yan, T.; Tian, Y.; Liu, S.; Xie, K.; Li, Z.; Wang, Y.; et al. ZmMs25 encoding a plastid-localized fatty acyl reductase is critical for anther and pollen development in maize. *J. Exp. Bot.* **2021**, *72*, 4298–4318. [CrossRef] [PubMed]
46. Lu, Y.; Cheng, X.; Jia, M.; Zhang, X.; Xue, F.; Li, Y.; Sun, J.; Liu, F. Silencing GhFAR3.1 reduces wax accumulation in cotton leaves and leads to increased susceptibility to drought stress. *Plant Direct.* **2021**, *5*, e00313. [CrossRef]
47. Guan, L.; Xia, D.; Hu, N.; Zhang, H.; Wu, H.; Jiang, Q.; Li, X.; Sun, Y.; Wang, Y.; Wang, Z. OsFAR1 is involved in primary fatty alcohol biosynthesis and promotes drought tolerance in rice. *Planta* **2023**, *258*, 24. [CrossRef]
48. Vioque, J.; Kolattukudy, P.E. Resolution and purification of an aldehyde-generating and an alcohol-generating fatty acyl-CoA reductase from pea leaves (*Pisum sativum* L.). *Arch. Biochem. Biophys.* **1997**, *340*, 64–72. [CrossRef]
49. Schwacke, R.; Schneider, A.; van der Graaff, E.; Fischer, K.; Catoni, E.; Desimone, M.; Frommer, W.B.; Flügge, U.I.; Kunze, R. ARAMEMNON, a novel database for *Arabidopsis* integral membrane proteins. *Plant Physiol.* **2003**, *131*, 16–26. [CrossRef]
50. Zhang, X.; Liu, Y.; Ayaz, A.; Zhao, H.; Lv, S. The plant fatty acyl reductases. *Int. J. Mol. Sci.* **2022**, *23*, 16156. [CrossRef]
51. Chen, W.; Yu, X.H.; Zhang, K.; Shi, J.; De Oliveira, S.; Schreiber, L.; Shanklin, J.; Zhang, D. Male Sterile2 encodes a plastid-localized fatty acyl carrier protein reductase required for pollen exine development in *Arabidopsis*. *Plant Physiol.* **2011**, *157*, 842–853. [CrossRef] [PubMed]
52. Dobritsa, A.A.; Shrestha, J.; Morant, M.; Pinot, F.; Matsuno, M.; Swanson, R.; Møller, B.L.; Preuss, D. CYP704B1 is a long-chain fatty acid omega-hydroxylase essential for sporopollenin synthesis in pollen of *Arabidopsis*. *Plant Physiol.* **2009**, *151*, 574–589. [CrossRef] [PubMed]
53. Doan, T.T.; Domergue, F.; Fournier, A.E.; Vishwanath, S.J.; Rowland, O.; Moreau, P.; Wood, C.C.; Carlsson, A.S.; Hamberg, M.; Hofvander, P. Biochemical characterization of a chloroplast localized fatty acid reductase from *Arabidopsis thaliana*. *Biochim. Biophys. Acta* **2012**, *1821*, 1244–1255. [CrossRef]
54. Shi, J.; Tan, H.; Yu, X.H.; Liu, Y.; Liang, W.; Ranathunge, K.; Franke, R.B.; Schreiber, L.; Wang, Y.; Kai, G.; et al. Defective pollen wall is required for anther and microspore development in rice and encodes a fatty acyl carrier protein reductase. *Plant Cell* **2011**, *23*, 2225–2246. [CrossRef]
55. Xu, G.; Guo, C.; Shan, H.; Kong, H. Divergence of duplicate genes in exon-intron structure. *Proc. Natl. Acad. Sci. USA* **2012**, *109*, 1187–1192. [CrossRef]

56. Rowland, O.; Zheng, H.; Hepworth, S.R.; Lam, P.; Jetter, R.; Kunst, L. CER4 encodes an alcohol-forming fatty acyl-coenzyme A reductase involved in cuticular wax production in *Arabidopsis*. *Plant Physiol.* **2006**, *142*, 866–877. [CrossRef]
57. Ma, J.; Deng, S.; Chen, L.; Jia, Z.; Sang, Z.; Zhu, Z.; Ma, L.; Chen, F. Gene duplication led to divergence of expression patterns, protein-protein interaction patterns and floral development functions of AGL6-like genes in the basal angiosperm *Magnolia wufengensis* (Magnoliaceae). *Tree Physiol.* **2019**, *39*, 861–876. [CrossRef]
58. Sornaraj, P.; Luang, S.; Lopato, S.; Hrmova, M. Basic leucine zipper (bZIP) transcription factors involved in abiotic stresses: A molecular model of a wheat bZIP factor and implications of its structure in function. *Biochim. Biophys.* **2016**, *1860*, 46–56. [CrossRef]
59. Fujita, Y.; Yoshida, T.; Yamaguchi-Shinozaki, K. Pivotal role of the AREB/ABF-SnRK2 pathway in ABRE-mediated transcription in response to osmotic stress in plants. *Physiol. Plant.* **2013**, *147*, 15–27. [CrossRef] [PubMed]
60. Marquis, V.; Smirnova, E.; Graindorge, S.; Delcros, P.; Villette, C.; Zumsteg, J.; Heintz, D.; Heitz, T. Broad-spectrum stress tolerance conferred by suppressing jasmonate signaling attenuation in *Arabidopsis* JASMONIC ACID OXIDASE mutants. *Plant J.* **2022**, *109*, 856–872. [CrossRef]
61. Yuan, M.; Shu, G.; Zhou, J.; He, P.; Xiang, L.; Yang, C.; Chen, M.; Liao, Z.; Zhang, F. AabHLH113 integrates jasmonic acid and abscisic acid signaling to positively regulate artemisinin biosynthesis in *Artemisia annua*. *New Phytol.* **2023**, *237*, 885–899. [CrossRef] [PubMed]
62. An, C.; Mou, Z. Salicylic acid and its function in plant immunity. *J. Integr. Plant. Biol.* **2011**, *53*, 412–428. [CrossRef] [PubMed]
63. Kidd, B.N.; Edgar, C.I.; Kumar, K.K.; Aitken, E.A.; Schenk, P.M.; Manners, J.M.; Kazan, K. The mediator complex subunit PFT1 is a key regulator of jasmonate-dependent defense in *Arabidopsis*. *Plant Cell* **2009**, *21*, 2237–2252. [CrossRef] [PubMed]